ELSEVIER

Scopus

doi

Journal of Vibration Engineering

ISSN:1004-4523

Registered

- SCOPUS
- GOOGLE SCHOLAR
- DIGITAL OBJECT IDENTIFIER (DOI)
- IMPACT FACTOR 6.1

Our Website
www.jove.science

Modal Analysis of a Truncated Magneto Electro Elastic Shells with Variable Boundary Conditions: A Numerical Investigation

Sudindra S[1](*), Dr. Anandkumar R. Annigeri[2], Dr. J S Srikantamurthy[3], and Dr. Raghavendra BV[4]

[1]Assistant Professor, Department of Mechanical Engineering,

BNM Institute of Technology, Bengaluru – 560070

[2]Professor, Department of Mechanical Engineering,

JSS Academy of Technical Education, Bengaluru – 560060

[3]Assistant Professor, Department of Mechanical Engineering,

JSS Academy of Technical Education, Bengaluru – 560060

[4]Associate Professor, Department of Mechanical Engineering,

JSS Academy of Technical Education, Bengaluru – 560060

Abstract

This paper presents a fully coupled Multiphysics finite element modal analysis of a Truncated Magnetoelectric Shell (TMEE) consisting of a Barium Titanate ($BaTiO_3$) piezoelectric layer and a Cobalt Ferrite ($CoFe_2O_4$) magnetostrictive layer arranged in a truncated cone (frustum) geometry. Simulations were performed in COMSOL Multiphysics 6.0 using simultaneous Solid Mechanics, Electrostatics, and Magnetic Fields physics interfaces. Four boundary conditions were investigated: Clamped-Clamped (CC), Clamped-Free (CF), Simply Supported-Clamped (SS-C), and Simply Supported-Simply Supported (SS-SS). Up to 8 Eigen frequencies were extracted for each case, and their 3D displacement-magnitude mode shapes were visualised on a revolved geometry. Results reveal an eigen spectrum spanning approximately 310–990 Hz across all four configurations. These findings offer comprehensive design guidance for tuning MEE shell resonance by selecting support conditions.

Keywords: *Modal analysis, Barium Titanate, Cobalt Ferrite ($CoFe_2O_4$), Eigenfrequency, COMSOL Multiphysics, Boundary conditions, Mode shapes.*

1. Introduction

Magnetoelectric (ME) composites that simultaneously exhibit piezoelectric and magnetostrictive coupling have attracted significant attention for applications in energy

harvesting, sensors, actuators, and vibration control. When such a material is formed into a shell structure, its resonant behaviour becomes highly sensitive to geometry and boundary conditions, making modal analysis a critical design step. Truncated conical (frustum) shells are widely used in aerospace and mechanical systems because the variable radius distributes stress more evenly than cylindrical shells. When the shell wall comprises magnetically and electrically active layers, structural vibrations couple to both electric and magnetic fields, yielding a rich eigenfrequency spectrum that cannot be predicted by purely mechanical models [1]. This work addresses this gap by performing a fully coupled three-physics (Solid Mechanics, Electrostatics, and Magnetic Fields) finite element analysis of a Truncated Magneto-Electro-Elastic (TMEE) frustum shell in COMSOL Multiphysics 6.0. Four distinct boundary conditions are studied, and up to eight eigenfrequencies with corresponding mode shapes are reported for each case.

2. Materials and Methodology

2.1 Structural Configuration

The MEE shell is modelled in 2D axisymmetric coordinates (r-z coordinates) using the Structural Mechanics and AC/DC modules in COMSOL Multiphysics 6.0. The computational domain spans radially from r ≈ 0.3 m to 1.01 m and axially from z = 0 to z = 3 m, forming a tapered frustum upon revolution about the symmetry axis. The frustum consists of two material domains. Domain 1 (inner region) is assigned to Barium Titanate ($BaTiO_3$), which acts as the piezoelectric layer, while Domain 2 (outer region) is assigned to Cobalt Ferrite ($CoFe_2O_4$), which provides the magnetostrictive response.

2.2 Material Properties

Table 1. summarises the key constitutive properties of the two materials. $BaTiO_3$ is a well-known piezoelectric ceramic with strong electromechanical coupling, while $CoFe_2O_4$ is a piezomagnetic material with significant magnetostrictive coefficients. The combination of these two layers in a bilayer frustum shell produces a magnetoelectric composite whose effective coupling is determined by the product of piezoelectric and piezomagnetic interactions.

Table 1. Material properties of the two shell layers.

Property	Barium Titanate ($BaTiO_3$)	Cobalt Ferrite ($CoFe_2O_4$)
Type	Piezoelectric (Ceramic)	Magnetostrictive (Ferrite)
Primary Coupling	Electro-mechanical	Magneto-mechanical
Physics Interface	Electrostatics (es)	Magnetic Fields (mf)
Role in Shell	Inner domain (Domain 1)	Outer domain (Domain 2)
Application	Sensing / Actuation	Energy harvesting / Sensing

2.3 Physics Interfaces and Boundary Conditions

2.3.1 Coupled Physics Interfaces

Three physics interfaces are simultaneously solved in this analysis:

(i) Solid Mechanics (solid) — governs structural deformation of the piezoelectric domain. (ii) Piezoelectric domains solve Gauss's law for electric potential V (iii) Magnetostrictive solves Ampère's law for the magnetic vector potential Aφ. All three physics are solved simultaneously using a consistent mass matrix formulation, ensuring that electromechanical and magneto-mechanical couplings are fully captured at every degree of freedom.

2.3.2 Boundary Condition Configurations

Four boundary condition configurations were applied to the top and bottom edges of the frustum shell. Table 2 summarises each configuration.

Table 2. Boundary condition configurations studied.

Case	Abbreviation	Bottom Edge	Top Edge
1	CC	Fixed Constraint (Clamped)	Fixed Constraint (Clamped)
2	CF	Fixed Constraint (Clamped)	Free (no constraint)
3	SS-C	Prescribed Displacement	Fixed Constraint (Clamped)
4	SS-SS	Prescribed Displacement	Roller

The CC case is the most constrained configuration, suppressing all translational and rotational degrees of freedom at both ends. The CF case resembles a cantilever, with the top edge left completely free. The SS-C and SS-SS cases represent intermediate levels of constraint, allowing rotation at one or both ends respectively.

3. Mesh and Element Type

3.1. Discretization

The 2D axisymmetric cross-section was discretised using COMSOL's physics-controlled free triangular mesh generator. 4-noded quadrilateral elements are employed across all three physics interfaces [2]. These six-node elements provide quadratic displacement interpolation with C^0 continuity, thereby mitigating shear locking in bending-dominated thin-walled frustum-shell modes. Table 3 summarises the element types for each interface.

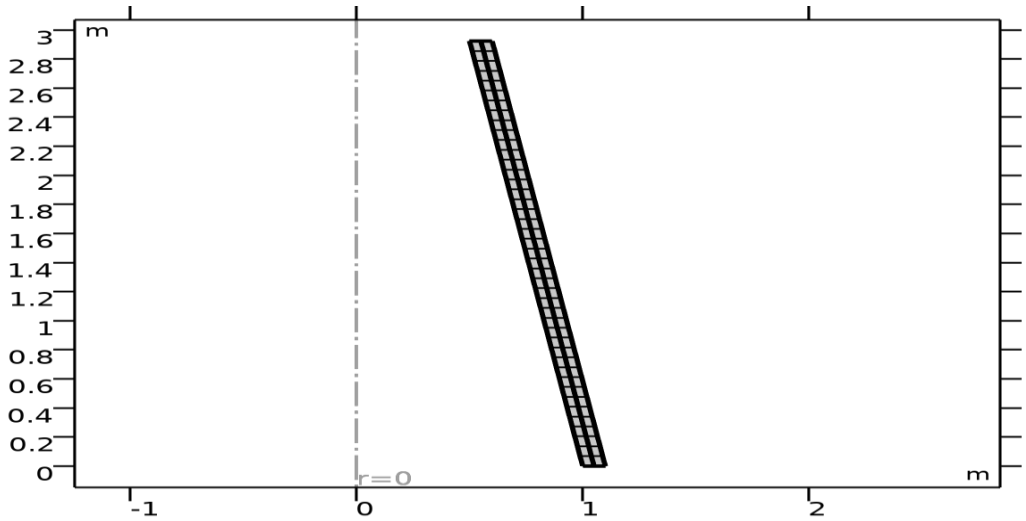

Figure 1. Showing a meshed 2-D Axisymmetric model composed of two layers

3.1.2 Element Type

COMSOL employs 4-noded quadrilateral elements throughout all physics interfaces. These four-node elements provide quadratic displacement interpolation with C^0 continuity [3]. The consistent mass matrix ensures frequency-independent accuracy for the first several modes. Table 3 summarises element types for each physics interface.

Table 3. Summary of element types for each physics interface

Physics Interface	Field Variable	Element Type
Solid Mechanics	Displacement (u, w)	4- Noded Quadrilateral
Electrostatics (es)	Electric Potential (V)	4- Noded Quadrilateral
Magnetic Fields (mf)	Magnetic Vector Potential Aφ	4- Noded Quadrilateral

4. Results and Discussion

Table 4. Eigenfrequency Results (Hz) for All Boundary Conditions

Mode	CC (Hz)	CF (Hz)	SS-C (Hz)	SS-SS (Hz)
1	542.73	413.04	310.56	311.66
2	686.96	526.23	526.23	526.23
3	795.03	702.56	702.56	702.56
4	841.61	754.44	727.67	776.12
5	882.67	826.9	754.44	795.03
6	894.53	834.6	776.37	826.90
7	900.66	875.51	826.90	875.15
8	936.2	894.53	841.61	896.98

4.1 Clamped-Clamped (CC)

Under the CC condition, both top and bottom edges are fully fixed, suppressing all translational and rotational degrees of freedom. This is the most constrained configuration and yields the highest fundamental eigenfrequency of 542.73 Hz among the four cases. Eight modes are captured, spanning 542.73 Hz to 936.20 Hz, exhibiting diverse shapes from simple first-bending to complex multi-lobe coupled deformation [4]. The CC eigen spectrum reveals a wide frequency spread, indicating that the double-clamped constraint generates a rich set of both bending-dominated low-frequency modes and membrane or torsional high-frequency modes.

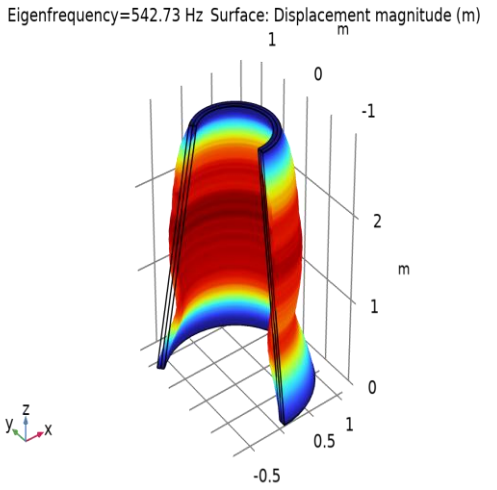

Figure 2. Fundamental Symmetric Bending Mode

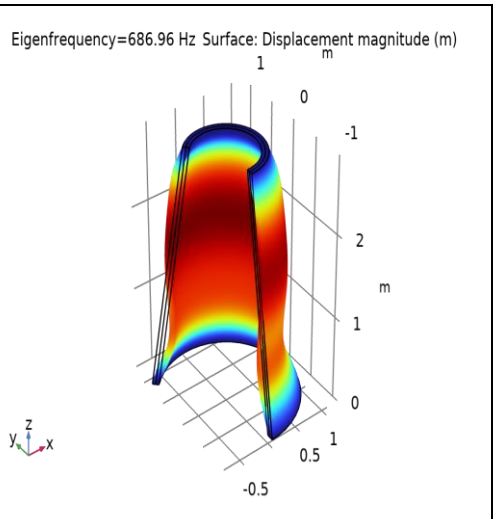

Figure 3. First Lateral Flexural Mode

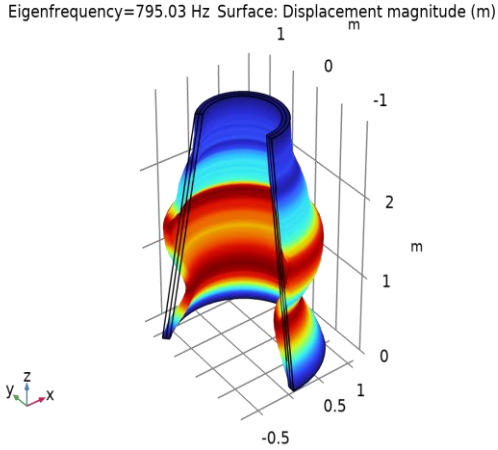

Figure 4. Second Axial Bending Mode (Two-Nodal Circle Mode)

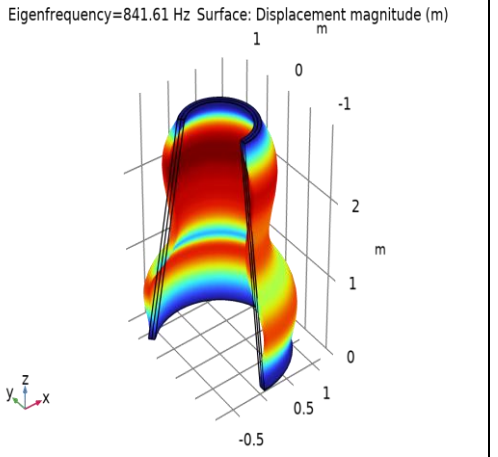

Figure 5. Axially Banded Standing-Wave Mode

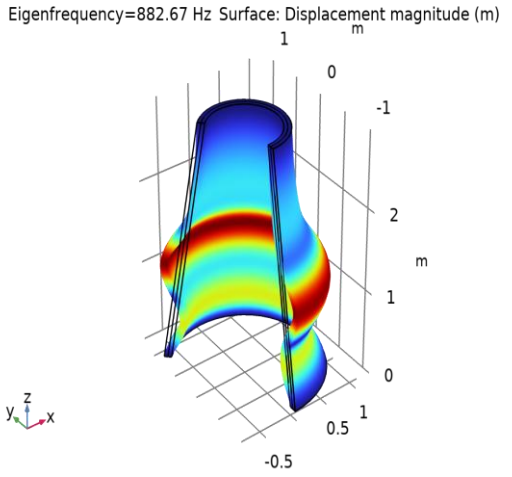

Figure 6. Circumferential Lobing Mode (n=1)

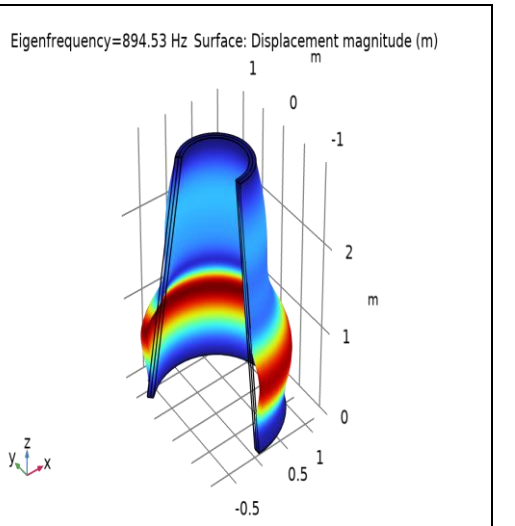

Figure 7. Membrane-Dominant Breathing Mode

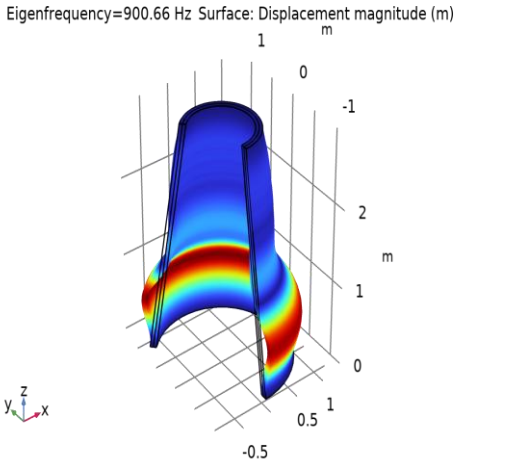

Figure 8. Torsional–Flexural Coupled Mode

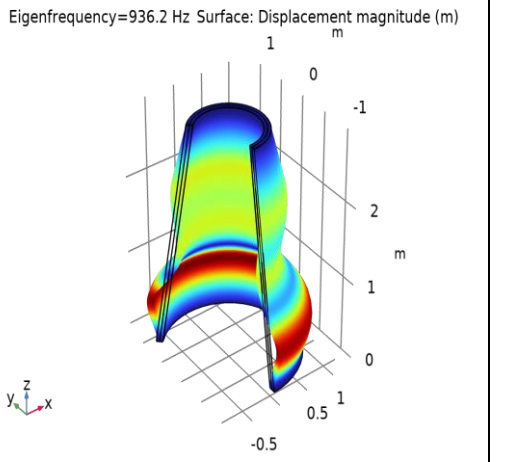

Figure 9. Higher-Order Multi-Lobe Shell Mode

4.2 Clamped-Free (CF)

The CF configuration clamps only the bottom edge, leaving the top edge completely free. This cantilever-type arrangement yields the second-highest fundamental frequency of 413.04 Hz [5]. Eight modes are extracted spanning 413.04 Hz to 1132.20 Hz, with a notably higher density of complex shell modes at upper frequencies. The CF fundamental mode displays the characteristic cantilever bending shape with maximum displacement at the free top and zero displacement at the clamped base. The absence of a top constraint substantially reduces rotational stiffness, lowering the fundamental frequency relative to the CC case by 129.69 Hz.

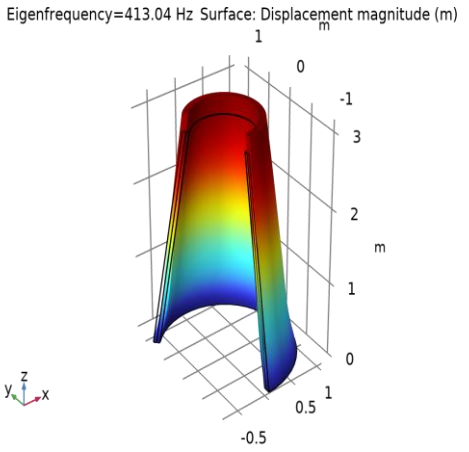

Figure 10. Cantilever Fundamental Bending Mode

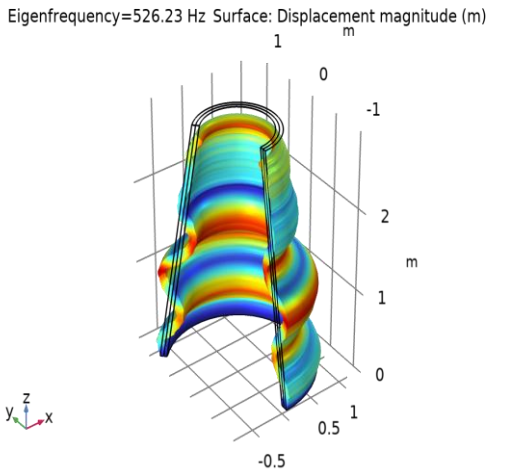

Figure 11. Axisymmetric Shell Breathing Mode

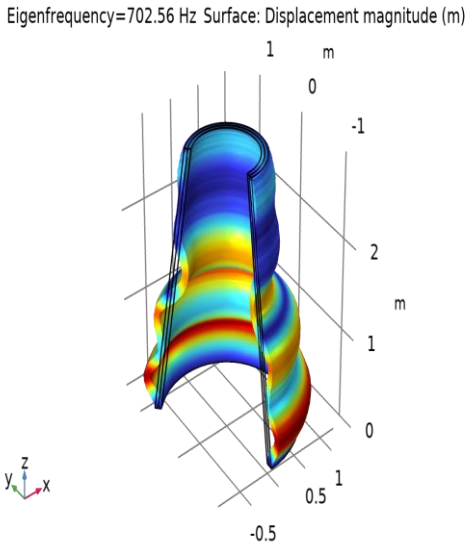

Figure 12. Membrane-Dominant Hoop Mode

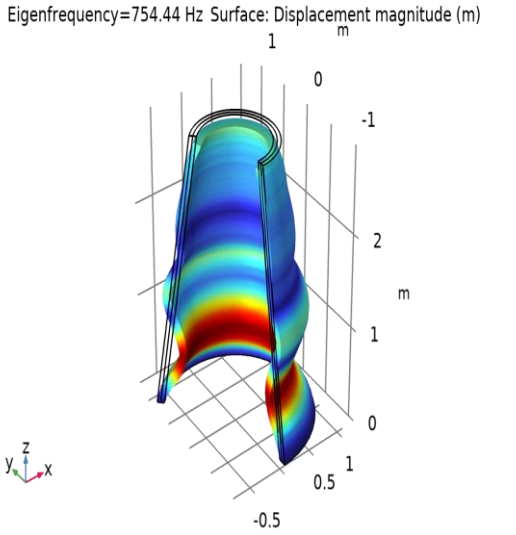

Figure 13. Base-Flare Radial Expansion Mode

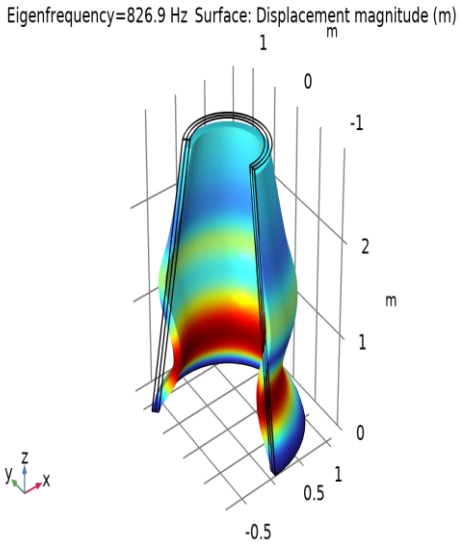

Figure 14. Axial–Circumferential Mixed Mode

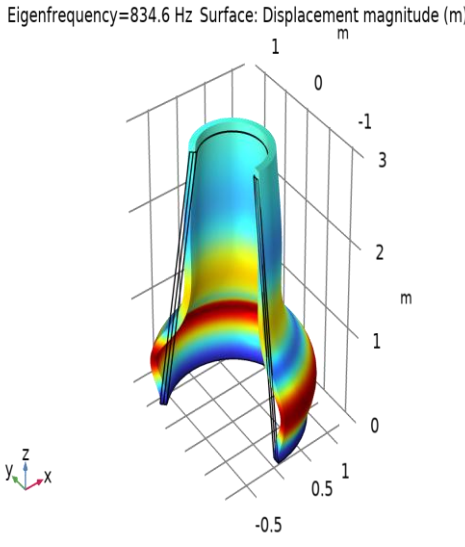

Figure 15. Two-Lobe Bending Mode (n=2)

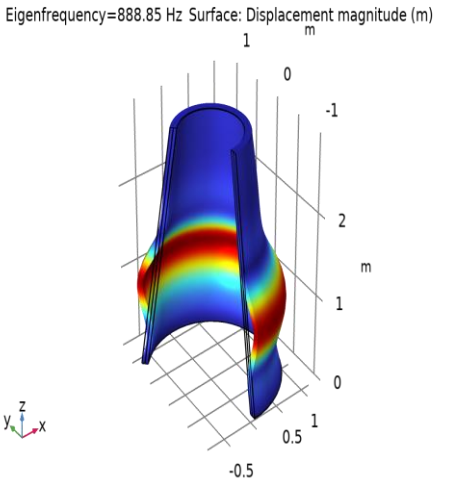

Figure 16. Circumferential Wave Mode (n=1)

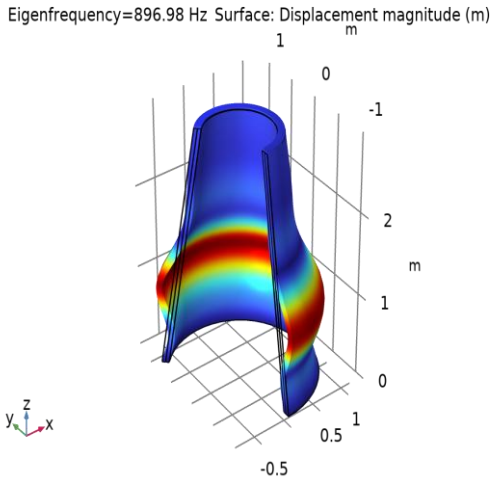

Figure 17. Higher-Order Flexural Mode

4.3 Simply Supported-Clamped (SS-C)

The SS-C case applies a prescribed displacement at the bottom (suppressing transverse displacement while permitting rotation) and a full fixed constraint at the top. This asymmetric combination yields a fundamental frequency of 310.56 Hz, the lowest of the four configurations [6]. Eight modes span 310.56 Hz to 983.71 Hz. The fundamental mode shows a half-sine displacement profile with a maximum at mid-height and near-zero displacement at both supported ends. The simply supported bottom edge dominates the fundamental frequency by removing the rotational constraint.

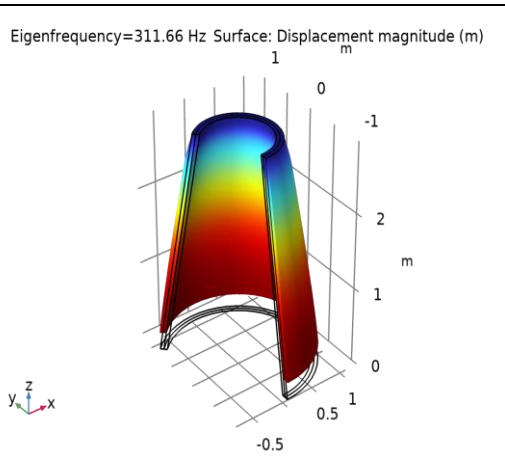

Figure 18. Half-Sine Simply Supported Bending Mode

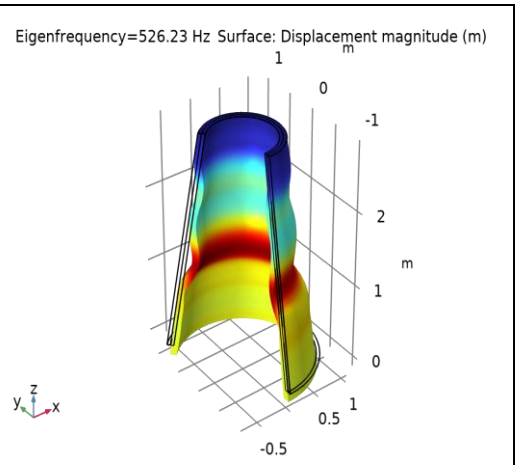

Figure 19.BC-Independent Breathing Mode

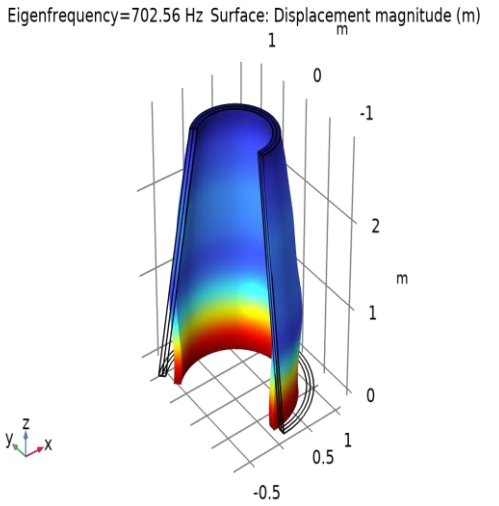

Figure 20. Circumferential Hoop Membrane Mode

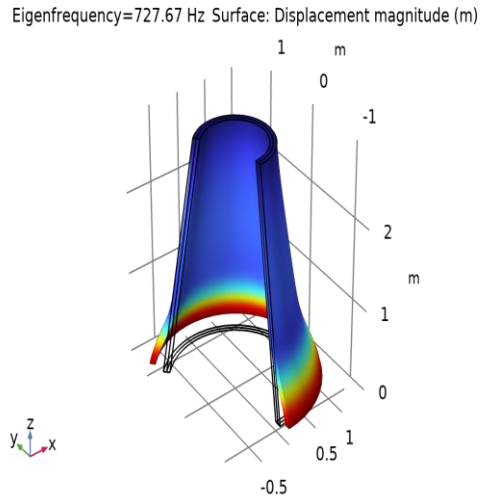

Figure 21. Base-Flare Membrane Mode

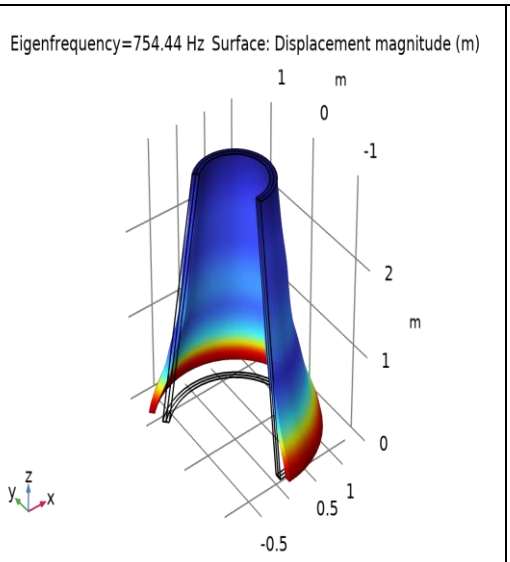

Figure 22. Helical Mixed Bending Mode

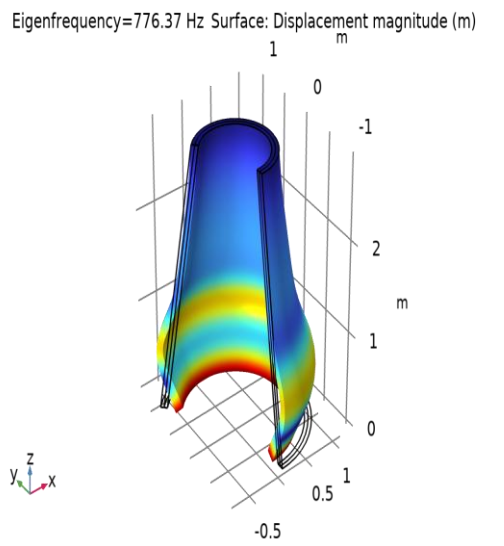

Figure 23.Axially Banded Mode

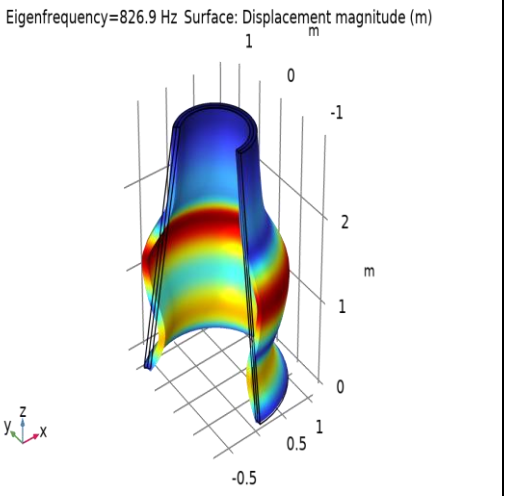

Figure 24. Two-Ring Bending Mode

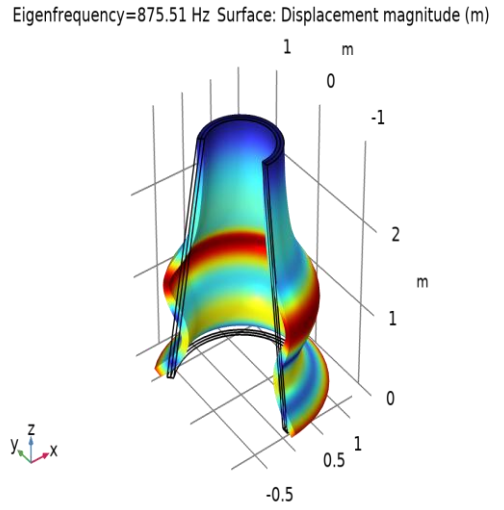

Figure 25. Circumferential Lobing Mode

4.4 Simply Supported-Simply Supported (SS-SS)

The SS-SS case uses a prescribed displacement at the bottom and a roller at the top, permitting rotation at both ends and axial movement at the top. This is the least constrained configuration, yielding a fundamental frequency of 311.66 Hz. Eight modes span 311.66 Hz to 967.88 Hz. The fundamental frequency differs from SS-C by only 1.10 Hz, confirming that both supported configurations exhibit nearly identical rotational freedom and hence similar lowest-mode stiffness. Higher modes converge on BC-independent membrane frequencies of 526.23 Hz and 702.56 Hz across all four boundary conditions, confirming the dominance of circumferential membrane stiffness in these modes [7].

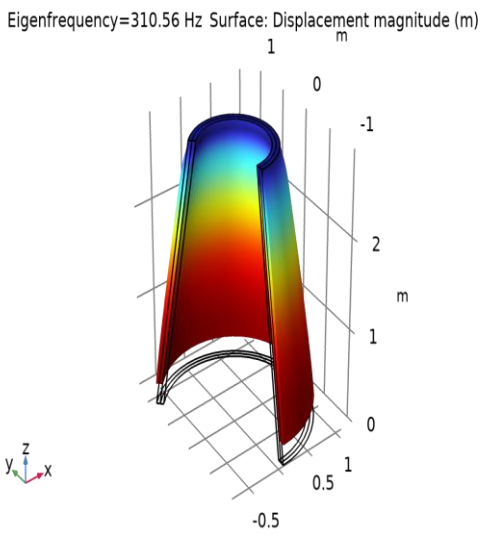

Figure 26. Symmetric Half-Sine Bending Mode

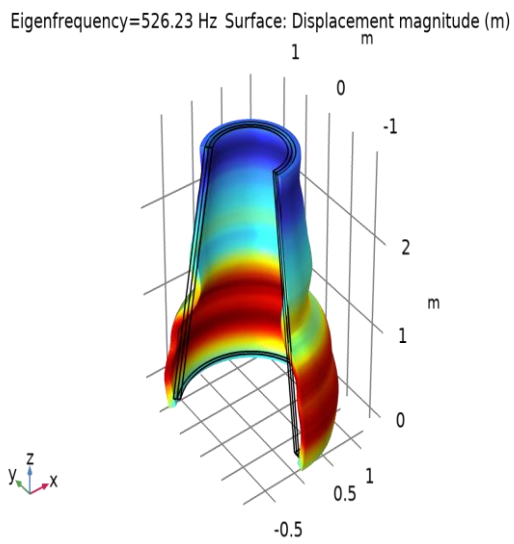

Figure 27. Axisymmetric Breathing Mode

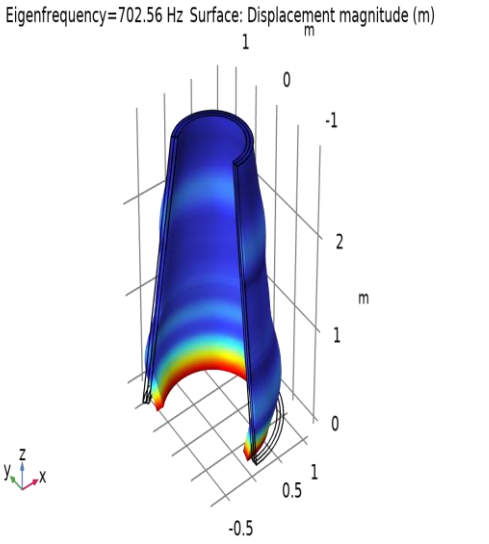

Figure 28. Hoop-Dominant Membrane Mode

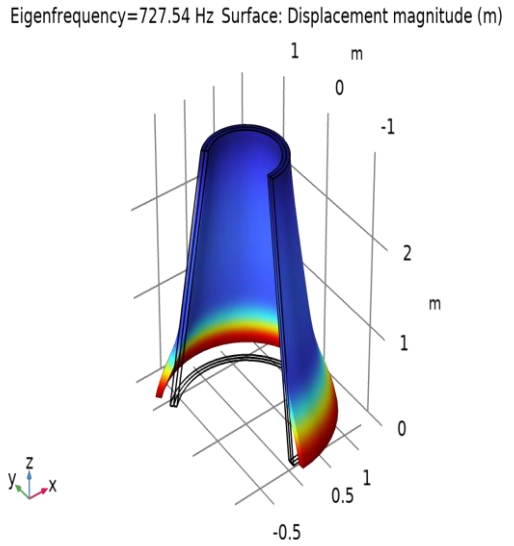

Figure 29. Second Bending Mode (Double-Bulge Mode)

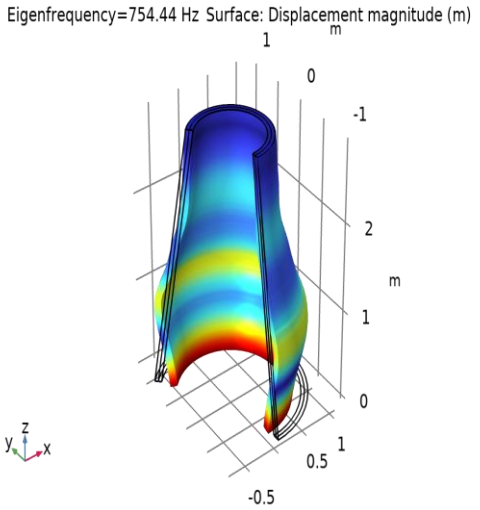

Figure 30. Axial Standing-Wave Mode

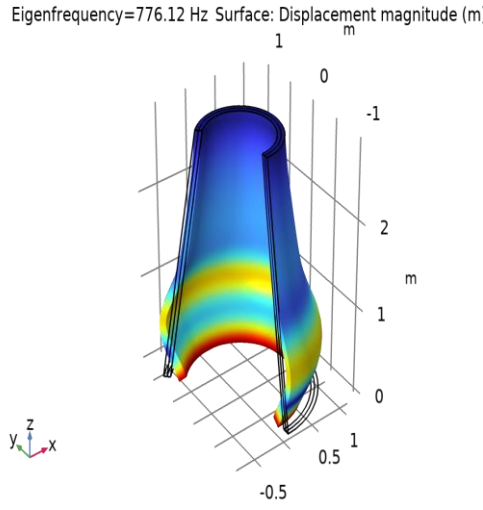

Figure 31. Circumferential Two-Lobe Mode

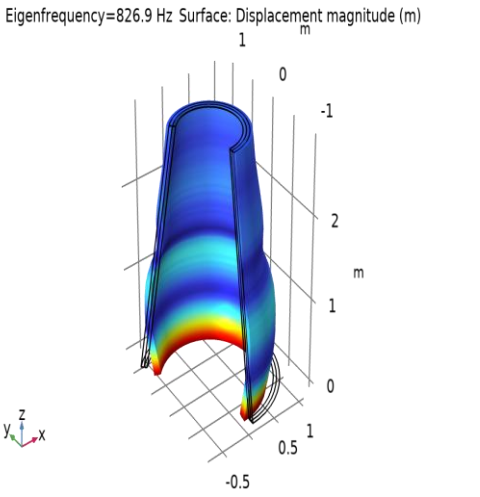

Figure 32. Higher-Order Shell Harmonic Mode

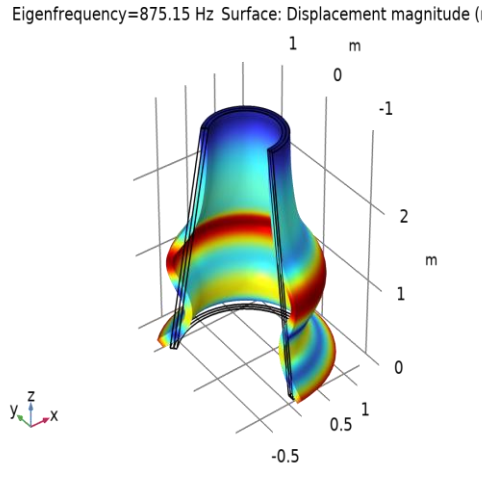

Figure 33. Flexural–Torsional Coupled Mode

4.5 Comparative Analysis

The fundamental frequencies across the four boundary conditions follow the expected trend:

CC (542.73 Hz) > CF (413.04 Hz) > SS-SS (311.66 Hz) ≈ SS-C (310.56 Hz)

This ranking is consistent with classical shell theory: greater constraint increases the effective bending stiffness, raising the fundamental frequency. The BC-independent membrane modes at 526.23 Hz and 702.56 Hz confirm that circumferential stiffness is geometry-driven and independent of end conditions, providing a useful invariant benchmark for validating models.

4.6 What Role Does the Smart Material Coupling Play?

The $BaTiO_3$ and $CoFe_2O_4$ layers are not just structural — they also resist bending through their electric and magnetic coupling. This makes the whole shell slightly stiffer than a plain elastic shell, raising all frequencies a little [8].

Barium Titanate ($BaTiO_3$) is a piezoelectric material: when it deforms, it generates an electric field that resists further deformation. This additional electrical stiffness contributes to the shell's total stiffness. Similarly, Cobalt Ferrite ($CoFe_2O_4$) is magnetostrictive: deformation generates a magnetic field that also resists deformation. Both effects act as invisible springs that add to the mechanical stiffness of the shell, shifting all eigenfrequencies upward compared to a purely mechanical shell of the same geometry.

5. Applications

The results of this study are directly useful in several real-world engineering areas. Because the shell's frequency can be tuned by changing only the support condition, and because [9]. the smart materials generate electricity and magnetic fields during vibration, TMEE shells are versatile devices.

The Shell Is Useful for Energy Harvesting and Sensing

Because $BaTiO_3$ generates electricity when it vibrates, a MEE shell resonating at its natural frequency can continuously convert ambient vibrations into electrical energy. By matching the shell's natural frequency to the dominant vibration of its environment (e.g., machinery at 500 Hz → use CC configuration), the shell becomes an efficient energy harvester [10]. The $CoFe_2O_4$ layer simultaneously acts as a magnetic sensor.

Medical and Wireless Applications Are Possible

Magnetoelectric materials can transfer power and signals wirelessly through biological tissue using magnetic fields — without wires or batteries. The stable membrane mode frequencies (526.23 Hz and 702.56 Hz) are ideal targets for wireless medical implants (pacemakers, drug delivery systems, neural stimulators) because they remain constant regardless of device position or body implantation.

Table 5. Applications in a wide frequency range

Application	Best BC	Frequency Range	How It Works
Energy Harvesting	CC / CF	413–543 Hz	Mount on industrial machines or bridges to collect electricity from vibrations
Vibration Sensors	All cases	310–990 Hz	Detect structural damage in aerospace panels, pipelines, buildings
Medical Ultrasound	CC higher modes	800–990 Hz	Compact imaging transducers; wireless power to implants
Noise Cancellation	SS-SS / SS-C	310–312 Hz	Active panels in car cabins or aircraft that cancel low-frequency noise

Application	Best BC	Frequency Range	How It Works
Smart Actuators	CC	542–936 Hz	Precision positioning in robotics; multi-frequency motion from one shell
Wireless Power Transfer	Any case	526 - 702 Hz	Stable membrane frequencies used as fixed reference for contactless charging

6. Conclusion

1. More Support = Higher Frequency

When both ends of the shell are fully clamped (locked), the shell vibrates at the highest fundamental frequency of 542.73 Hz. When both ends are simply supported (free to rotate), the frequency drops to 311.66 Hz. This happens because clamping adds stiffness — a stiffer shell vibrates faster, just like a tightly stretched guitar string produces a higher pitch than a loose one.

2. Clamped-Free Acts Like a Cantilever

When only the bottom end is clamped, and the top is left free (CF case), the shell behaves like a diving board or a flagpole. The fundamental frequency is 413.04 Hz — lower than the fully clamped case (CC) by 130 Hz, because one free end allows the shell to bend more easily. This is the classic cantilever effect well-known in mechanical engineering.

3. Simply Supported Cases Are Almost Identical

The SS-C (310.56 Hz) and SS-SS (311.66 Hz) fundamental frequencies differ by only 1.10 Hz. This is because once one end is allowed to rotate freely (simply supported), the vibration stiffness is already low. Adding support at the other end also adds very little extra flexibility. The weakest boundary condition dominates the fundamental frequency.

4. Two Frequencies Never Change Regardless of Support

Modes at 526.23 Hz and 702.56 Hz appeared at the same frequency in all four boundary-condition cases. These are called membrane modes — the shell wall vibrates in a circular (hoop) pattern. Since this type of vibration depends only on the shell's geometry and material stiffness not the end supports the frequencies remain constant no matter how the shell is mounted.

5. Up to 8 Vibration Modes Were Found Per Case

Each boundary condition produced up to 8 distinct natural frequencies and mode shapes, ranging from simple bending (a single bulge) to complex multi-lobed patterns. Higher modes involve more waves along the shell's height and circumference, engaging membrane and torsional stiffness in addition to bending stiffness [11]. More constraint (CC) produces a richer set of modes within a narrower frequency range.

6. Piezoelectric Layer ($BaTiO_3$) Stiffens the Shell Electrically

When Barium Titanate bends, it generates an electric voltage. This voltage creates an internal electric force that resists further bending — acting like an invisible extra spring. This electromechanical coupling raises all the natural frequencies slightly above what a plain elastic shell would have. It also changes the bending mode shapes because the stiffness is not uniform — it depends on the direction of electric polarisation.

7. Magnetostrictive Layer ($CoFe_2O_4$) Stiffens the Shell Magnetically

When Cobalt Ferrite deforms, it generates a magnetic field. This magnetic field resists further deformation through magneto mechanical coupling, adding magnetic stiffness on top of the mechanical stiffness. This effect is particularly strong during membrane (hoop) deformation, which is why the $CoFe_2O_4$ layer directly influences the BC-independent membrane modes at 526 Hz and 702 Hz.

8. Combined Coupling Creates Unique Mode Shapes

When both $BaTiO_3$ and $CoFe_2O_4$ are active together, some vibration modes are fully coupled — the shell deforms mechanically while simultaneously generating both electric and magnetic fields [12]. These magneto-electro-elastic coupled mode shapes are unique to this type of shell and cannot be predicted by a purely mechanical simulation. Ignoring the coupling would result in incorrect frequencies and mode shapes.

9. Frequency Can Be Tuned by Over 625 Hz Without Changing Material

The total frequency range spanned across all four boundary conditions is from 310.56 Hz (SS-C fundamental) to 936.20 Hz (CC Mode 8) — a range of over 625 Hz. This entire range is accessible simply by changing how the shell ends are supported, without altering the material composition, shell thickness, or geometry. This is a powerful and low-cost design tool for engineers.

Acknowledgments

The authors acknowledge the computational resources and facilities provided by I-STEM (Indian Science, Technology, and Engineering facilities Map) for conducting this research. The finite element analyses were performed using COMSOL Multiphysics software version 6.0 with the AC/DC and MEMS modules.

REFERENCES

The following references were used as the scientific basis for this study:

[1] Priya, S. & Inman, D. J. (Eds.) (2009). Energy Harvesting Technologies. Springer, New York.

[2] Beeby, S. P., Tudor, M. J. & White, N. M. (2006). Energy harvesting vibration sources for microsystems applications. Measurement Science and Technology, 17(12), R175

[3] Fiebig, M. (2005). Revival of the magnetoelectric effect. Journal of Physics D: Applied Physics, 38

[4] Ehrenstein, W., Mathur, N. D. & Scott, J. F. (2006). Multiferroic and magnetoelectric materials. Nature, 442(7104), 759–765.

[5] Jaffe, B., Cook, W. R. & Jaffe, H. (1971). Piezoelectric Ceramics. Academic Press, London.

[6] Engdahl, G. (Ed.) (2000). Handbook of Giant Magnetostrictive Materials. Academic Press, San Diego.

[7] Nan, C. W., Bichurin, M. I., Dong, S., Viehland, D. & Srinivasan, G. (2008). Multiferroic magnetoelectric composites. Journal of Applied Physics, 103(3), 031101.

[8] COMSOL AB. (2023). COMSOL Multiphysics Reference Manual, Version 6.0. COMSOL AB, Stockholm.

[9] COMSOL AB. (2023). Structural Mechanics Module User's Guide, Version 6.0. COMSOL AB, Stockholm

[10] Berlincourt, D. A., Curran, D. R. & Jaffe, H. (1964). Piezoelectric and piezomagnetic materials. Physical Acoustics, 1A, 169–270

[11] Olabi, A. G. & Grunwald, A. (2008). Design and application of magnetostrictive materials. Materials & Design, 29(2), 469–483

[12] Meirovitch, L. (2001). Fundamentals of Vibrations. McGraw-Hill, New York.